DECOVALEX-2023
Task E Specification
Revision 0

Spent Fuel and Waste Disposition

Prepared for
US Department of Energy
Spent Fuel and Waste Science and Technology

Kristopher L. Kuhlman
Sandia National Laboratories

April 23, 2020
SAND2020-4289 R

DISCLAIMER

This information was prepared as an account of work sponsored by an agency of the U.S. Government. Neither the U.S. Government nor any agency thereof, nor any of their employees, makes any warranty, expressed or implied, or assumes any legal liability or responsibility for the accuracy, completeness, or usefulness, of any information, apparatus, product, or process disclosed, or represents that its use would not infringe privately owned rights. References herein to any specific commercial product, process, or service by trade name, trade mark, manufacturer, or otherwise, does not necessarily constitute or imply its endorsement, recommendation, or favoring by the U.S. Government or any agency thereof. The views and opinions of authors expressed herein do not necessarily state or reflect those of the U.S. Government or any agency thereof.

Sandia National Laboratories is a multimission laboratory managed and operated by National Technology and Engineering Solutions of Sandia LLC, a wholly owned subsidiary of Honeywell International Inc. for the U.S. Department of Energy's National Nuclear Security Administration under contract DE-NA0003525.

Sandia National Laboratories

SUMMARY

This report is the Task E specification (revision 0) for DECOVALEX-2023. Task E is focused on understanding thermal, hydrological, mechanical and chemical (THMC) processes, especially related to predicting brine migration in heated salt. The main test case being used is the ongoing Brine Availability Test in Salt (BATS) heater test located underground at the Waste Isolation Pilot Plant (WIPP) in Carlsbad, New Mexico. This report provides short motivational background, a summary of relevant experiments and data, and a step-by-step plan for the analysis by the teams participating in Task E (Rev. 0 includes detailed description of steps 0 and 1). This document will be revised, and more detail will be added to later steps during DECOVALEX-2023.

Report Version Number	Date	
SAND2020-4289R (rev 0)	April 23 2020	April 2020 kickoff meeting

ACKNOWLEDGEMENTS

The author thanks Alex Bond and Jens Birkholzer of the DECOVALEX project, the teams participating in the task, and thanks to Sandia reviewers Ernie Hardin, Rick Jayne, Melissa Mills, and Emily Stein. The BATS experiment itself wouldn't be possible without the WIPP facility and its personnel (thanks to George Basabilvazo, Andy Ward, and Sean Dunagan), the WIPP Test Coordination Office (Doug Weaver, Brian Dozier, and Shawn Otto), nor the team of people across Sandia, Los Alamos, and Lawrence Berkeley national laboratories designing, implementing, troubleshooting, and interpreting the experiment.

CONTENTS

ACRONYMS

BATS	brine availability test in salt
CT	computed tomography
DECOVALEX	DEvelopment of COupled models and their VALidation against Experiments
DOE	Department of Energy
DOE-EM	DOE Office of Environmental Management
DOE-NE	DOE Office of Nuclear Energy
DOPAS	full-scale Demonstration Of Plugs And Seals
DRZ	disturbed rock zone
EDZ, EdZ	Excavation Damaged Zone, Excavation disturbed Zone
GRS	Gesellschaft für Anlagen- und Reaktorsicherheit
LANL	Los Alamos National Laboratory
LBL	Lawrence Berkeley National Laboratory
SFWST	Spent Fuel and Waste Science & Technology (DOE-NE program)
SNL	Sandia National Laboratories
TH^2MC	thermal, two-phase hydrological, mechanical, and chemical (also TH^1, TH^2M, TH^2C)
US	United States
WIPP	Waste Isolation Pilot Plant (DOE-EM site)

VARIABLES AND PARAMETERS

k	permeability [m^2]
k_r	relative permeability [-]
p_c	capillary pressure [Pa]
t	time [sec]
T	temperature [ºC]
ϕ	porosity [-]
σ_r, σ_θ	radial and azimuthal stress [Pa]
S_e	relative water (brine) saturation [-]

DECOVALEX-2023 TASK E SPECIFICATION

This specification is for the teams participating in Task E. It provides a motivational background and describes the steps involved. This document will be updated, as needed, during the duration of Task E.

1. Introduction

The DECOVALEX program is generally interested in coupled processes (i.e., thermal, hydrological, mechanical, and chemical – THMC) relevant to radioactive waste disposal in geologic formations. Task E participants seek to understand and predict coupled processes which impact brine availability in bedded salt deposits under heated conditions associated with disposal of heat-generating waste in a salt repository. Brine can impact repository long-term performance by corroding metal waste forms and packages, mobilizing radionuclides from the repository to the biosphere, and providing mechanical resistance to eventual drift creep closure.

Bedded and domal salt deposits have been considered as candidate host media for radioactive waste disposal since the topic was first investigated in the 1950s. Geologic salt deposits possess a suite of favorable properties (Table 1) for repository-scale long-term waste isolation (scale: 10^3 m and 10^6 yr), but these same salt formations also present some complexities to many standard characterization and numerical modeling approaches at shorter length and time scales (10^1 m and 10^1 yr). Many complicating issues are related to the extent, nature, and evolution of the excavation damaged zone (EDZ) around rooms and boreholes, where the salt material properties have locally changed. The EDZ is surrounded by a larger excavation disturbed zone (EdZ), where relevant state variables have changed (Davies & Bernier, 2005; Hansen, 2003). Stormont et al. (1991) instead use the roughly equivalent terminology "major" and "minor" disturbed rock zone (DRZ).

Figure 1 illustrates how porosity (ϕ) is associated with the damage derived from the differential stress state around an excavation. The EDZ is the primary source of ϕ and permeability (k) in salt. There are several steep and non-uniform gradients of material properties and state variables across the EDZ (i.e., between the excavation and intact rock in the far field), which strongly impact gas and liquid migration.

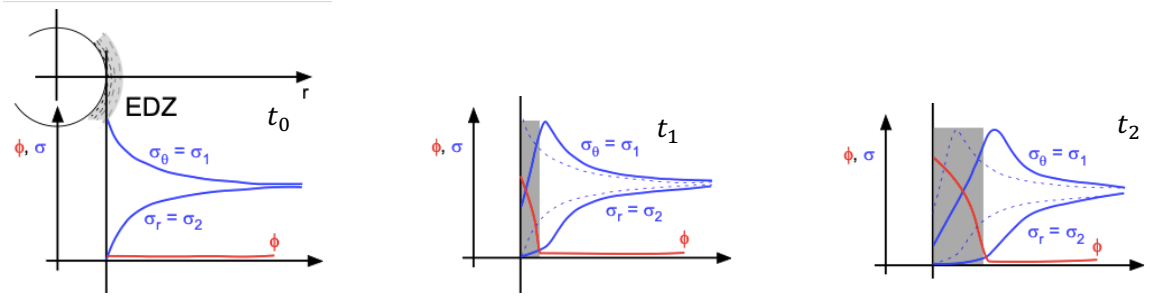

Figure 1. Schematic of damage (porosity, ϕ) development in an EDZ around an idealized borehole or room, illustrating radial (σ_r) and tangential (σ_θ) stress through time ($t_0 < t_1 < t_2$) (Popp, 2019).

The data used in Task E to explore THMC processes in bedded salt come from the Waste Isolation Pilot Plant (WIPP). Some data are historical, from investigations in the 1980s and 1990s, while much of the data comes from the ongoing brine availability test in salt (BATS). Some examples are also drawn from other historic brine migration experiments at other underground salt facilities, including Avery Island (salt dome in Louisiana), Asse (salt dome in Germany), and Project Salt Vault (bedded salt in Kansas).

Table 1. High-level Summary of Salt Behaviors and Properties.

Salt property	Long-term benefits	Possible complicating factors
Creep closure & healing	Eventual drift closure and healing of excavation damaged zone (EDZ) to undisturbed conditions	Drift openings are deforming and require maintenance; creep accelerates with increasing temperature (T); large strain viscoplastic creep is more complex to model than purely elastic behavior.
Thermal conductivity	Higher thermal conductivity keeps max T at waste packages lower	Thermal conductivity decreases with increasing T.
Near-zero undisturbed permeability (k)	No far-field regional brine flow	EDZ fractures are main source of k; EDZ is anisotropic and graded; fractures are more complex than porous media; low k can support high pressure gradients, including thermal pressurization; T expansion increasing confinement and interacts with EDZ fractures (k can decrease with increasing T).
Near-zero undisturbed porosity (ϕ)	Most ϕ is associated with fractures in EDZ, and creep closes them readily	EDZ fractures are main source of ϕ; EDZ is graded; higher-ϕ EDZ is gas-filled, while brine fills far-field ϕ (i.e., a brine saturation (S_e) gradient).
Salt is relatively dry	Less brine available for corrosion & radionuclide transport, and dry salt tolerates a higher maximum repository temperature	Minor fluid inclusions, clay, and hydrous minerals are significant contributors to total brine. These atypical brine components may require complex models/source terms in flow and transport models.
Evaporite minerals are very soluble in water, which is T-dependent	Significant salt precipitates near heat sources, filling voids. High ionic strength of brine reduces biological and radiological (e.g., criticality) concerns	Condensing steam dissolves salt, boiling brine precipitates salts (both change salt ϕ and k). Hot salt may dissolve into in situ brine (solubility increases with increasing T).

The primary Task E objective is to predict and quantify the importance of coupled THMC processes relating to the availability of water to flow into heated excavations in bedded salt. Increased brine flow from and through salt occurs due to increased ϕ and k in the EDZ around excavations (Figure 2). Brine migration is sensitive to the distribution and evolution of ϕ and k (Figure 3), which decrease going away from excavations (Beauheim & Roberts, 2002). Porosity in the EDZ is mostly due to micro- and macro-fractures attributed to damage accumulation. Micro-fractures can close readily under increased confining stress due to thermal expansion (and fractures can re-open after these stresses are relieved when a heat source is suddenly turned off). Hydrological observations are being used to indirectly observe the effects of mechanical deformation on the near-drift environment.

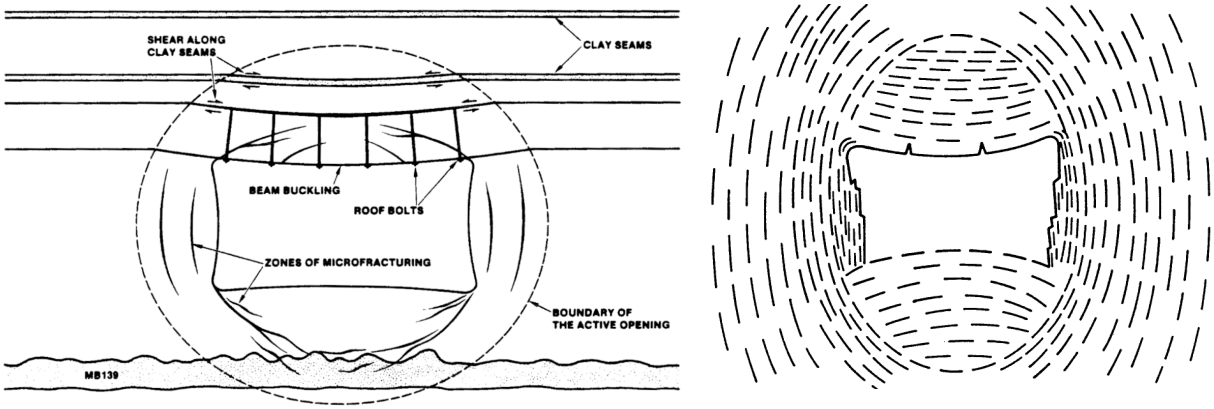

Figure 2. Schematic of EDZ and fractures near salt excavations (Borns & Stormont, 1988a; 1988b).

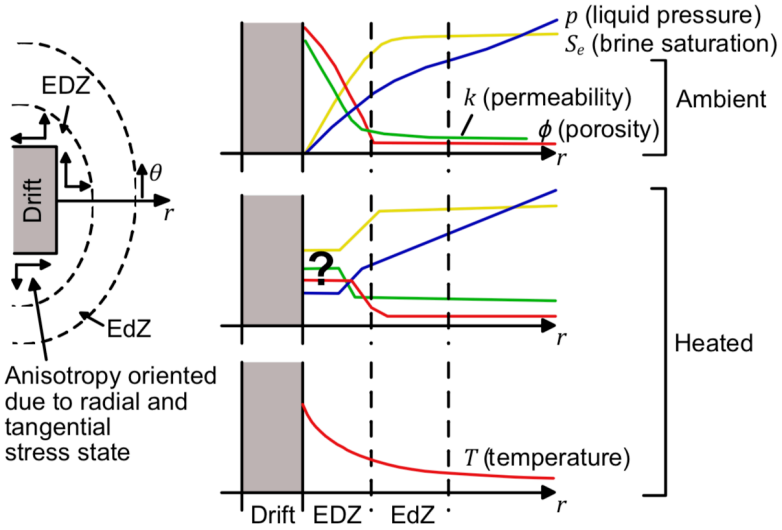

Figure 3. Schematic trends in hydrological properties and state variables from an excavation in salt to the far field under ambient (top) and heated (bottom) conditions.

Brine is found in several distinct forms in bedded evaporites at WIPP (Figure 4). Arranged from greatest to least contribution of overall water, they are:

1. Pore-water in disseminated clay (< 5 vol-% non-uniformly in evaporites (< 1 vol-% in BATS test interval); clay can be 25 vol-% brine)
2. Intragranular brine within salt grains ($\sim 1 - 2$ vol-% in salt crystals)
3. Hydrous minerals, including pre-existing ones (e.g., polyhalite $K_2Ca_2Mg(SO_4)_4 \cdot 2H_2O$, the most significant mineral in the BATS test interval after halite) and precipitate from brine evaporation (e.g., bischofite, epsomite, & kieserite)
4. Intergranular brine between salt grains ($\ll 1$ vol-% undisturbed, ϕ and water content are higher in EDZ after redistribution of brine)

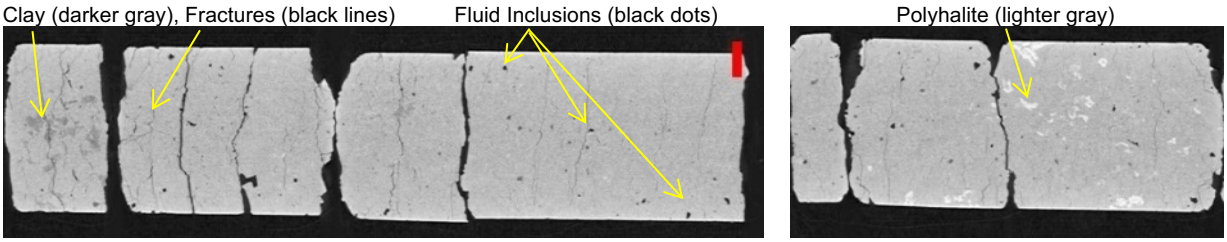

Figure 4. Brine types observed in BATS core CT data (20 mm scale; Betters et al., 2020).

Original or healed intergranular porosity often appears microscopically as a network of small grain-boundary fluid inclusions, while EDZ-derived intergranular porosity appears as small open fractures. Intergranular brine is the least significant overall source of initial brine in the WIPP bedded salt system, but the network of damage enhanced EDZ porosity is the primary pathway for brine or vapor to reach a borehole or excavation. The other brine types (hydrous minerals and intracrystalline fluid inclusions) must flow into the intergranular porosity network to transport through the EDZ.

These brine types have different spatial distributions in the evaporites (related to deposition and alteration), and their different natures means they will respond differently to pressure and temperature gradients. Fluid inclusions have been observed to move under a temperature gradient; they can migrate to the intergranular porosity, where they will then migrate as liquid or gas under a pressure gradient. These water types may have different chemical compositions (Kuhlman et al., 2018; Section 2), and stable water

isotope composition. In WIPP bedded salt, discrete cm- to m-scale clay and anhydrite layers produce much more brine than does halite with minor disseminated clay. These mapped layers include Marker Bed 139 and Clay F (Figure 5), which are typically intersected in vertical boreholes at WIPP (Nowak & McTigue, 1987). To avoid these mapped non-salt layers, the BATS field test was completed in horizontal boreholes confined to a single horizon of mostly (≥ 95 %) halite.

2. Experiments

We discuss in more detail two historical unheated experiments at WIPP, and the ongoing BATS heated brine migration test. The two ambient-temperature WIPP experiments were performed in the 1990s and have been presented in previous reports. The small-scale brine inflow experiment (Finley et al., 1992) monitored brine production soon after drilling boreholes and provided data for the historic INTRAVAL model comparison study (Beauheim et al., 1997). The small-scale mine-by experiment (Stormont et al., 1991) observed the evidence of damage around a 96.5-cm diameter borehole through gas and brine permeability tests at different radial distances, comparing before and after excavation.

2.1 Small-Scale Brine Inflow Experiment (INTRAVAL)

Finley et al. (1992) presented brine inflow data collected from boreholes at WIPP immediately after drilling. Two near-horizontal boreholes (90-cm diameter L4X01 and 10-cm diameter L4B01) were completed in the argillaceous halite of Map Unit 0 (MU-0) in Room L4 soon after mining the room. MU-0 is stratigraphically just below the BATS test interval (Map Units 1–3; Figure 5). The data series (weekly or monthly brine inflow totals from the day after completion) from the smaller-diameter L4B01 and some vertical boreholes that did not intersect Marker Bed 139 were utilized most successfully in INTRAVAL.

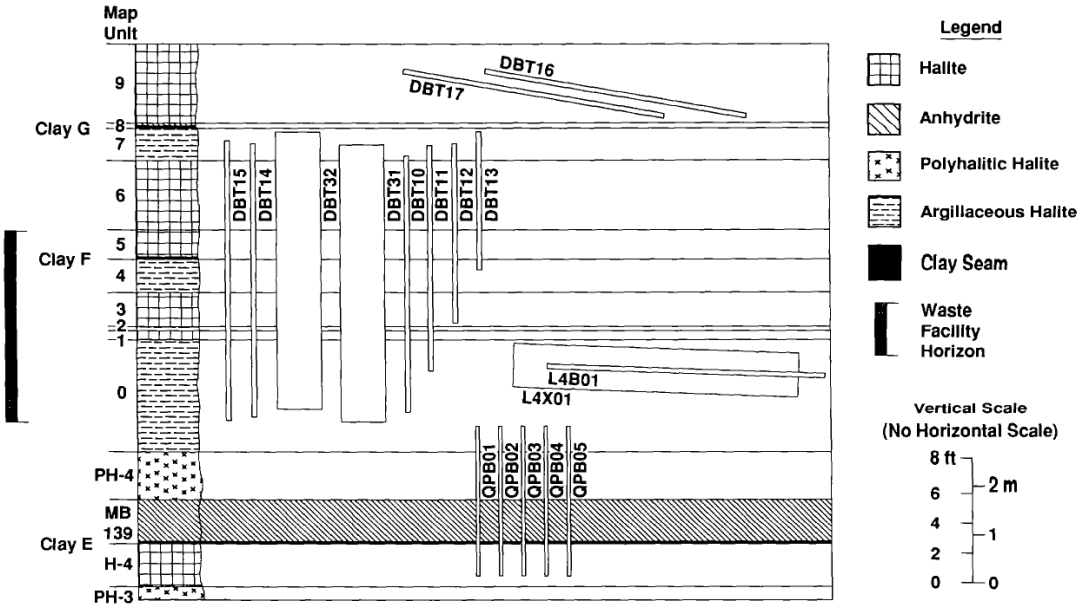

Figure 5. Idealized WIPP stratigraphy and small-scale brine inflow boreholes (Finley et al., 1992).

The goal in the INTRAVAL "WIPP 1" test case was to establish the applicability of Darcy's Law to brine flow through WIPP evaporites under a pressure gradient (Beauheim et al., 1997). Three international teams analyzed the unheated borehole brine inflow data and found Darcy flow to be approximately valid, with fits associated with parameters in the range $10^{-21} \leq k \leq 10^{-22}$ m^2.

The data from the Small-Scale Brine Inflow experiment (described in Finley at al., 1992; McTigue, 1993; and Beauheim et al., 1997) available electronically to the team members (i.e., Finley et al., 1992;

Appendix E); see details regarding data distribution in Section 4. These data will be analyzed by participating teams as a benchmarking exercise in step 0.

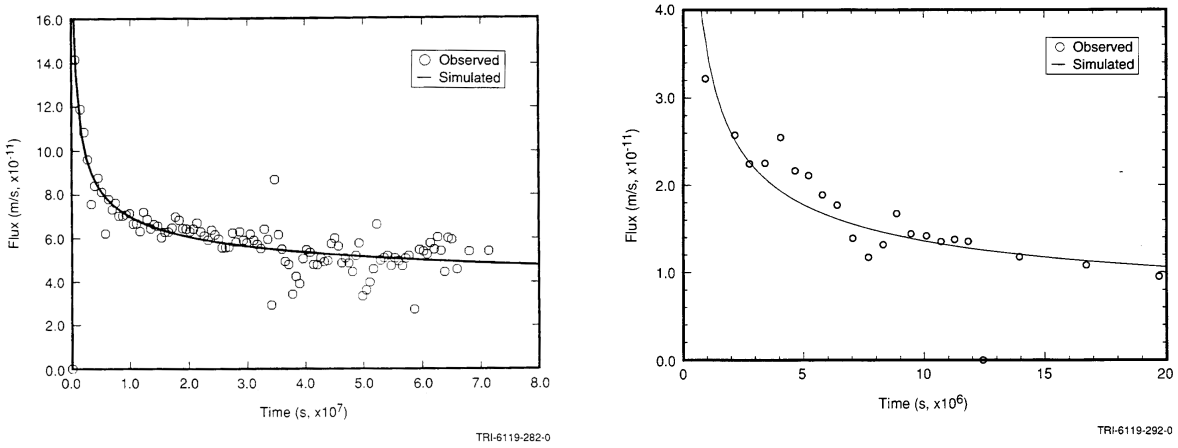

Figure 6. Unheated small-scale brine inflow results, fit by analytical solutions (McTigue, 1993), in INTRAVAL report (Beauheim et al., 1997). Vertical borehole DBT11 (left) intersected Clay F, while horizontal borehole L4B01 (right) is completed in MU-0.

More brine inflow data (including brine composition) are available for other boreholes at WIPP, reported in several Brine Sampling and Evaluation Program reports prepared by the WIPP site contractor (e.g., Deal et al., 1995). Borehole OH23 was a 46-m long horizontal borehole completed in MU-0 for which data are also available from soon after its completion (Kuhlman et al., 2017; Appendix A-1).

2.2 Small-Scale Mine-by Experiment

Stormont et al. (1991) presented data characterizing the Excavation Damaged Zone (EDZ) and Excavation disturbed Zone (EdZ) surrounding a 96.5-cm diameter borehole. The data from the mine-by experiment include gas and brine permeability test data, before and after drilling a large-diameter vertical borehole between the monitoring boreholes. The study provides a basis for understanding the extent of changes in porosity, k, and brine saturation surrounding an excavation at WIPP. The data and results are summarized in Stormont et al. (1991). Figure 7 summaries the study's results, including the inferred DRZ extent, and the gas saturation extent, outside of which relative gas permeability is effectively zero. The EDZ salt porosity is brine-saturated in the far field, but as damage accumulates and the porosity increases, the brine no longer saturates the increased porosity and since the damage happens quickly (minutes to hours), there is no time for brine to flow in from the far-field to fill the newly created porosity.

Data from the small-scale mine-by experiment are not explicitly used as a test case for model comparison in Task E, but the test and its results are mentioned here explicitly due to its significant relevance to interpreting BATS and the small-scale brine inflow test cases.

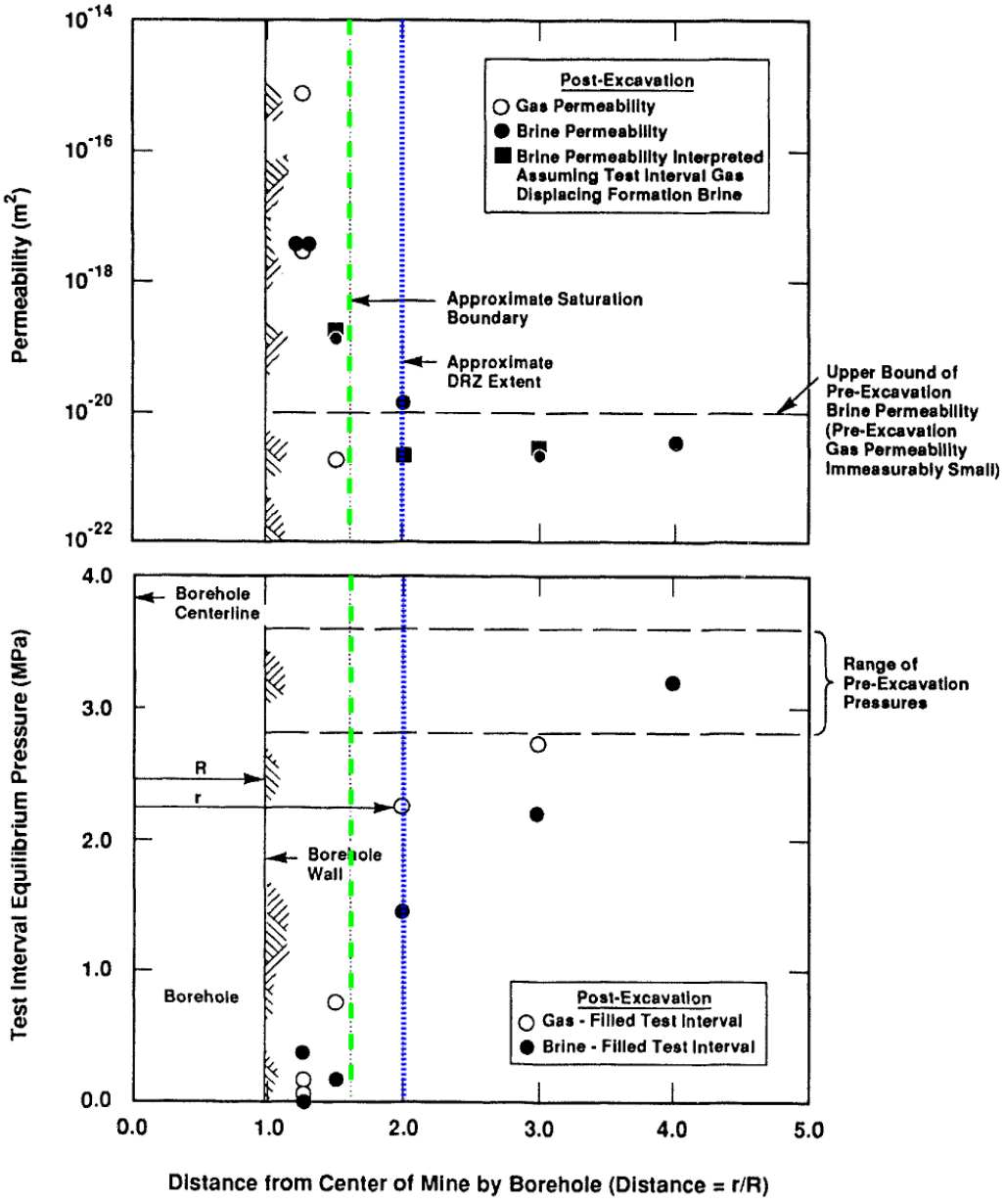

Figure 7. Interpretation of *k* and static formation pressure from small-scale mine-by experiment (Fig 24 Stormont et al., 1991), summarizing EDZ extent around 96.5-cm borehole.

2.3 Heated Brine Availability Test in Salt (BATS)

BATS is one part in a sequence of field tests relevant to heat-generating nuclear waste planned at the WIPP (Stauffer et al., 2015; Johnson et al., 2017; Mills et al., 2019). By April 2020, there are two complete phases to the BATS test at WIPP. A preliminary "shakedown" test (Boukhalfa et al., 2019; Guiltinan et al., 2020) was conducted in summer 2018 to compare heater designs and test equipment in the salt environment, completed in boreholes cored in 2013 (BATS "1s"). Brine inflow was quantified by circulating dry N_2 gas behind a packer and through desiccant (i.e., grams water per day) and temperature data (thermocouples) were collected during several sequential multi-day heating episodes at different heater power levels. These results provide a dataset to test numerical modeling approaches (Johnson et al., 2019; Guiltinan et al., 2020).

After several months of experimental setup, a second test was conducted from January to March 2020 with a source borehole maintained at ~96 ºC (2 weeks pre-heating data, 1 month heated data, 2 weeks cool-down data). This test was conducted in boreholes drilled specifically for the BATS test (Mills et al., 2019), with a significantly larger observation dataset collected across two similar nearby arrays (heated and unheated). More BATS heater test phases are planned in 2020 and 2021 using these boreholes, and these data will also be part of Task E (once COVID-19 related travel restrictions are lifted from those participating on the experimental side). Subsequent tests in the same boreholes will be conducted at higher heater power levels and with additional data collection (e.g., gas permeability packer test results at multiple temperatures, and breakthrough data from liquid/gas tracer tests).

Once testing in the current borehole arrays is complete (possibly 2021), 30-cm diameter post-test cores will be collected from the test bed (between HP, D, SM and SL boreholes, Figure 8) to measure the distribution of introduced liquid tracers (fluorescent dye and anionic perrhenate), analyze any microstructural changes in salt or brine distribution due to heating, and analyze the salt/brine/cement interfaces surrounding the seals test (SL borehole).

Laboratory tests are currently underway (April 2020) at SNL and LANL to characterize the brine content and material properties of the samples from salt cores and grout used to install instrumentation. Thermal conductivity, heat capacity, electrical resistivity, sonic velocity, and *k* will be measured across a range of relevant temperatures (30 to150 ºC) for samples of salt cores and grout for thermocouples and electrodes.

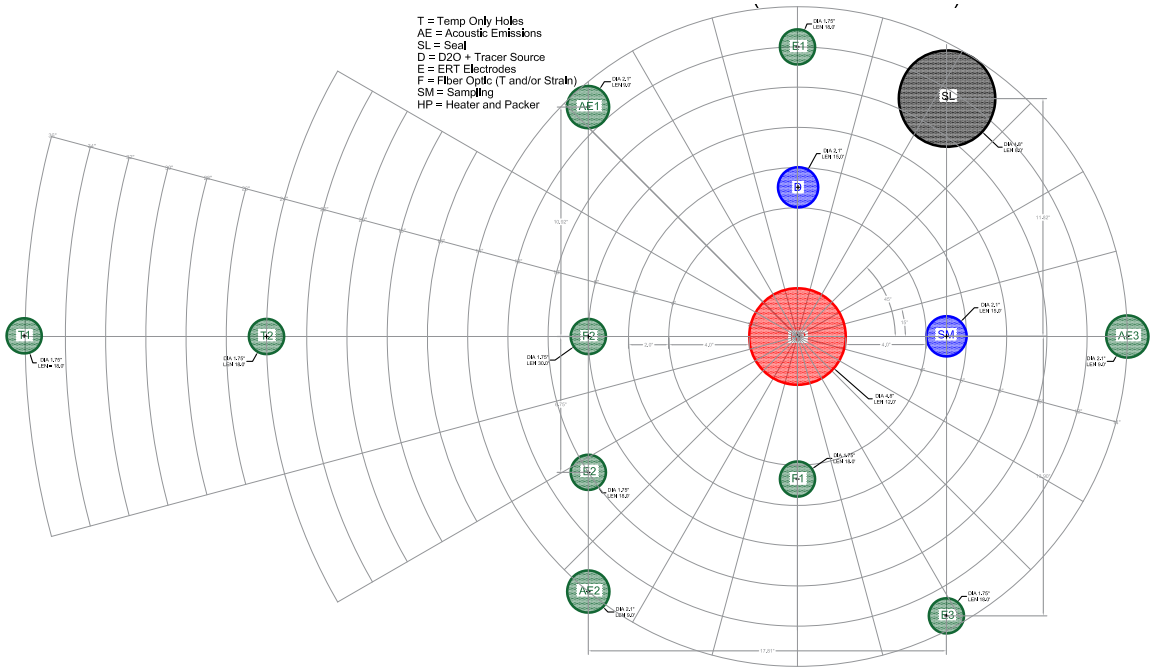

Figure 8. Pattern of horizontal boreholes in each BATS array (heated and unheated).

The January to March 2020 episode of the BATS test had the following data available from 14 boreholes (Figure 8, Figure 9, Table 2) in each heated and unheated array:

- A central packer-isolated borehole [HP] with dry N_2 gas flowing behind the packer to remove moisture flowing into the central borehole. Circulated gas was routed from these boreholes to in-drift monitoring and measurement of:
    - Gas stream temperature, pressure, flowrate and relative humidity (15 min. intervals)
    - Water isotope composition (i.e., $\delta^{18}O$ and $\delta^{2}H$) via cavity ringdown spectrometer (2 min.)

  - Gas stream composition (e.g., O_2, N_2, H_2O, Ar, CO_2) via quadrupole mass spec. (5 min.)
  - Total mass water produced by weighing desiccant (~2× weekly)
- Borehole closure is monitored in the heated and unheated HP boreholes via a displacement-monitored spring-steel centralizer (15 min.)
- Temperature data; 2 strings of 16 thermocouples grouted into boreholes [T1 & T2], in addition to other thermocouples co-located with other instruments (15 min.)
- Electrical resistivity tomography (ERT) surveys conducted once daily at night (3 strings of 18 ERT electrodes grouted into boreholes [E1-E3])
- Acoustic emission (AE) events from continuous monitoring (3 strings of multiple piezoelectric sensors pushed against the borehole wall with de-centralizers [AE1-AE3])
- Laboratory-prepared cement seals (Sorel cement and salt-based Portland cement) with embedded strain gages and thermistors placed in boreholes [SL] behind mechanical packers, monitoring strain, cement temperature, and temperature/humidity of packer-isolated interval (15 min.)
- Fiber optic distributed temperature and strain data recorded on 2 sets of fibers grouted into 2 boreholes [F1 & F2] (hourly)
- Liquid samples collected from adjacent packer-isolated borehole [SM] (attempted weekly)
- Tracer injection borehole (not used in Jan-Mar 2020 test) [D]

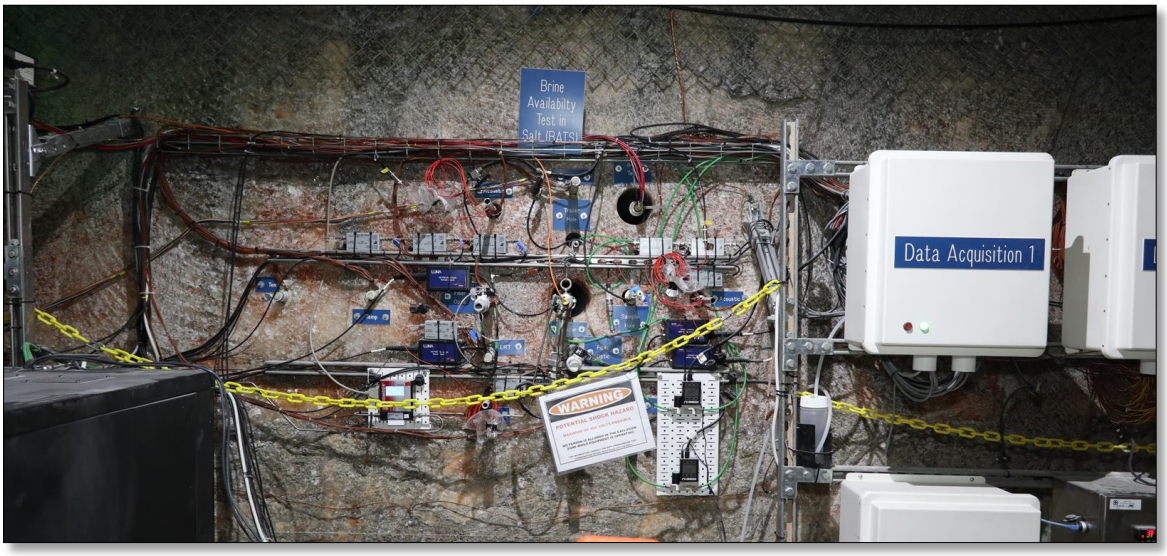

Figure 9. BATS heated array at the beginning of Jan-Mar 2020 testing.

To complement ongoing laboratory work and the BATS field test, Gesellschaft für Anlagen- und Reaktorsicherheit (GRS) is setting up poromechanical lab experiments. This lab work will build on previous cement sealing work in salt as part of the Full-scale Demonstration of Plugs and Seals (DOPAS) project (Czaikowski et al., 2016). GRS will conduct triaxial lab permeability test using coaxial prepared samples of salt from WIPP and cement seals, similar to those emplaced in SL boreholes in BATS. These hydromechanical tests will test the stability of salt/cement/brine interfaces in the system, under a range of conditions similar to and also beyond those expected in the BATS field test, in the lab.

Table 2. Types of data collected (or planned) from heated and unheated BATS arrays.

Processes	BATS Data
Thermal	Heater power [HP heated borehole]; thermocouple temperature (grouted in [T, E boreholes], in air [HP, AE, SL, SM boreholes]); temperature along grouted fiber [F boreholes]; lab estimates of thermal conductivity & heat capacity on core samples (+ grout).
Hydrological	Core CT image data; SEM and TGA analyses on pre- and post-tests core samples; pre-test packer gas permeability test results; brine production via N_2 [HP boreholes]; ERT-interpreted Δ electrical conductivity; liquid and gas tracer tests [D, SM, HP boreholes]; lab permeability tests on core samples; lab brine imbibition tests on core samples; lab analyses of fluid inclusions in pre- and post-test core samples; lab permeability of seals (GRS).
Mechanical	borehole closure [heated and unheated HP boreholes]; 3-axis strain in cement plugs [SL boreholes]; estimated timing and location of acoustic emissions due to thermal stresses [AE boreholes]; strain observations along grouted fiber [F boreholes]; drift closure measurements (since 2013); lab estimates of ultrasonic wave velocity in core samples (+ grout).
Chemical	Gas composition of N_2 stream [HP heated and unheated boreholes]; stable water isotopes in N_2 stream [HP boreholes]; liquid brine samples for lab analyses of composition [SM boreholes]; gas and liquid tracer samples [D, SM, HP boreholes]; lab analyses on post-test cores, including over-cored cement seals (heated and unheated); post-test samples of salts precipitated in HP boreholes; lab analyses of interfaces in seal system (GRS).

3. Proposed Task Structure

Task E will incorporate elements of:

- **Benchmarks:** Relatively simple simulations, either synthetic or well-constrained experiments to act as a 'warm-up' for participants and allow codes and process models to be compared.
- **Test Cases:** More complex modeling, with detailed comparisons against field and laboratory experimental data.
- **Uncertainty and Parameter Sensitivity:** Quantification of model-data uniqueness and model parameter sensitivity helps build understanding to balance complexity of added processes and non-linearities.

In this document single-phase and two-phase hydrological behavior in THMC models will be differentiated as TH^{1}MC and TH^{2}MC (Kuhlman, 2019), as this distinction arises often in Task E.

The overall objective of Task E is to use data from past and ongoing field and laboratory experiments to build and refine conceptual models of physical processes relevant to brine availability in bedded salt. Given the highly coupled nature of THMC processes in salt (Kuhlman & Malama, 2013; Kuhlman, 2014; Kuhlman, 2019), it seems prudent to begin with "uncoupled" datasets (i.e., unheated brine flow, heat conduction through salt) and comparison against published analytical solutions for coupled physics (i.e., McTigue, 1986; 1990).

Brine inflow conditions for the BATS test are complicated by the two-phase nature of brine flow in damaged salt. The jump from single-phase brine flow to two-phase brine and vapor flow is a significant step up in complexity, and there is scant data available to parameterize two-phase flow in fractured salt. Uncertainty associated with two-phase flow should be understood before including the additional complications of heating, so this stage is called out separately. To parameterize two-phase flow in the EDZ (i.e., capillary pressure ($p_c = p_{\text{air}} - p_{\text{brine}}$) and relative permeability (k_r) changes with brine saturation, S_e) we will need to leverage a range of experimental and literature sources.

To match both the heating and cooling portions of the brine inflow data from the heated BATS array will require changes to k related to changes in confining stress (Lai, 1971; Stormont & Fuenkajorn, 1993), since changes in stress are driven by changes in temperature (confined thermal expansion). Exploring the importance, nature, and possible implementation of this coupling during heating and cooling is a primary goal of Task E. The impacts of two-phase flow are even more important during heating phases, because there will often be a phase change around the heater (temperature in the region around the heater borehole will get above boiling in planned BATS tests), surface tension can be a function of temperature, and the compressible gas phase in the EDZ pore space reduces the effects of thermal pressurization.

The later portions of the task will involve several possible pathways, depending on the interests of the participants:

- The addition of brine and precipitated salt chemistry, stable water isotopes, precipitation and dissolution of salt to change ϕ and k, and the effects of different sources of brine on the brine response (e.g., fluid inclusion migration under a temperature gradient or dehydration of clay at elevated temperature) are advanced non-linear hydrological effects for analyses.
- The coupled inversion of geophysical data (e.g., daily ERT tomograms shows change in resistivity or inferred source timing and location of acoustic emission events) to constrain THMC modeling is another optional advanced analysis.
- The study of cement seals, specifically salt/brine/cement interactions in both the lab (i.e., planned GRS laboratory experiments) and field (ongoing data collection from BATS SL boreholes and subsequent post-test over-core analyses) relies on interpretation of temperature and brine

production data, but will include interpretation of geochemical, mineralogical, and poromechanical testing that will only become available partway through the task.

- The effects of creep in salt on brine production. Creep is most important in long-term predictions, but creep is significantly accelerated by higher temperatures. Creep is driven by deviatoric stresses around excavations (i.e., drifts, boreholes, and fractures) and works to close them. Closing microfractures EDZ porosity, possibly altering ϕ, k, and S_e even during shorter tests.

Working with simpler datasets, conceptual models, and benchmarks first allows adding complexity as it is needed, and understanding the importance of different mechanisms (e.g., physical coupling and non-linear behaviors) under different conditions (e.g., unheated, heated, variable number of fluid-phases). Building complexity and performing uncertainty quantification at each step will be important to make meaningful predictions in the final application stage.

At any step in the task, there will be a balance between including physical process complexity and constitutive law non-linearities; including dimensional, geometric, and heterogeneity-based complexity; and understanding the effects of complexity using parameter estimation, uncertainty quantification and sensitivity analysis (which may profit from quick-running models).

The following structure is proposed for Task E:

Step 0: Single-process H^1 and T benchmarks

- Simulate single-phase brine production into at least three boreholes in salt using the ambient temperature brine inflow data from the WIPP small-scale brine inflow test (Finley et al., 1992), following a procedure similar to the INTRAVAL comparison (Beauheim et al., 1997). From the available data, choose boreholes with brine inflow histories showing a monotonically decreasing brine inflow rate.

- Simulate temperature distribution due to conduction from a constant-temperature borehole heat source for at least five thermocouple locations during the Jan-Mar 2020 BATS heating and cooling cycle (unpublished data). Teams will be provided changes in temperature data through time, laboratory estimates of thermal properties, and relevant coordinates and distances between the source and measurement points. Depending on the length of the record considered, it may be important to include the effects of the access drift, any open or grouted boreholes, and irregularities in the power level in the first hours of the test.

- Estimate parameter uncertainty and model parameter sensitivity for these two benchmarks. Once a model has been fitted to data, provide some measure of key parameter uncertainty. Parameter sensitivity estimates should be made near the optimal model-data fit. One outcome will be to illustrate relative importance (i.e., sensitivity) of key model parameters through time.

Step 1: TH^1 benchmarking and H^2M/H^2 unheated brine inflow (BATS test case)

- Benchmark against single-phase brine production to a heated borehole, matching the published analytical solution of McTigue (1990) along space and time profiles, using properties given for salt in Table 1 of McTigue (1986). For this synthetic benchmark, provide sensitivity of model parameters to observations through time and quantify impacts from any non-linear behaviors captured in numerical models but not included in the analytical solution (e.g., brine viscosity or thermal conductivity varying with T). Compare the match between numerical and analytical models in both space and time with and without available non-linear effects turned on in the numerical model.

- Parameterize multi-phase flow in salt. Justify the choices of two-phase flow parameters in salt (i.e., both the functional form chosen and any required parameters). Illustrate the range of choices of models and parameters in plots of p_c and k_r vs. S_e. Few two-phase flow data exist for a

fractured-salt EDZ. Examples for possible two-phase flow characterization include model inversion of laboratory brine imbibition tests on BATS salt cores, estimation from X-ray computed tomography (CT) scans of BATS cores (Betters et al., 2020), or literature survey including using analogous non-halite WIPP rocks or oilfield rocks with existing data (e.g., Howarth & Christian-Frear, 1997; Davies, 1991). This parameterization is key to (and part of) the next bullet, but it is mentioned separately since it is a non-trivial part of the step from H^1 to H^2.

- Simulate H^2M/H^2 brine production in a borehole under multi-phase ambient conditions, predicting gradients in pressure and saturation across the EDZ. Brine production data will be provided from boreholes in the unheated BATS array. The results of this H^2M/H^2 simulation are the initial conditions for the TH^2M heated BATS test case (step 2). EDZ parameter distributions in H^2 simulations will be specified, while H^2M simulations may predict damage, ϕ, and k directly. Provide estimates of parameter uniqueness and parameter sensitivity through time.

Step 2: TH^2M multi-phase brine inflow through a heated EDZ and TH^2MC tracer tests (BATS test case)

- Simulate brine production in a borehole in salt under multi-phase heated conditions (including production changes during heating and cooling), building on previous steps. Brine production in the heated BATS array through time, including after turning off the heater, will be provided. Borehole and laboratory gas permeability test data for salt at different temperatures will be provided. The effects of thermal expansion on the stress, ϕ, and k of the salt (i.e., closing and opening of EDZ microfractures) should somehow be included in models. Provide estimates of uniqueness parameter uniqueness and parameter sensitivity through time. Do two-phase models make better predictions than single-phase models?

- ***Optional:*** Simulate H^2C gas and liquid tracer advection, matching breakthrough times between source (D) and observation (SM & HP) boreholes in the *unheated* BATS array. Provide uncertainty quantification and sensitivity of relevant model transport parameters.

- ***Optional:*** Simulate TH^2MC gas and liquid tracer advection, matching breakthrough times between source (D) and observation boreholes (SM & HP) boreholes in the *heated* BATS array. Provide uncertainty quantification and sensitivity of relevant model transport parameters.

Step 3: Simulate more advanced TH^2MC coupled processes in BATS test case (***choose alternatives***)

- Step 3a: Simulate TH^2M brine production while using geophysical data as constraints. Using time-lapse ERT and/or AE timing and source location estimates, constrain TH^2M brine production estimates from step 2. ERT results show changes in resistivity, which can be related to changes in brine content (given changes in resistivity with temperature are estimable) from steps 1 and 2. AE events reveal the timing and location of cracking in the salt, which can constrain or confirm predicted changes in k due to changes in σ in step 2. Compare the parameter uncertainty and sensitivity estimates from previous steps.

- Step 3b: Predict TH^2MC cement seal behavior in lab/field. Predict (i.e., no field seal permeability data exist to compare against) permeability of the confined borehole salt/cement system in heated and unheated SL boreholes from observed temperature, strain, and post-test compositional analyses. GRS will provide poromechanical lab test results (including permeability of a salt/seal/brine system) using WIPP salt and brine, along with similar cement recipes. Present uncertainty in model parameters and sensitivity of key parameters to observations through time.

- Step 3c: Simulate TH^2MC brine production with additional geochemical processes. Brine production estimates from step 2 will be updated to include one or more of the following H-C effects: distribution and behavior of different water sources (i.e., fluid inclusions, clay dehydration) in multi-phase brine inflow predictions; effects from precipitation and dissolution of salt effects on ϕ and k; brine composition data (e.g., ionic content of produced brine from

different water sources); mineralogical and water content of precipitated salts; non-condensable gas composition of produced gas stream; and isotopic composition of produced water. Comparisons will be made against predictions in step 2, including parameter uncertainty associated with new parameters and sensitivity of key parameters through time.

- Step 3d: Simulate TH^2M brine production with creep. Creep closure in salt is driven by and works to reduce differential stresses. Creep becomes more significant at longer time scales, higher deviatoric stresses, and higher temperatures. This additional mechanism should either be considered explicitly in coupled viscoplastic numerical models or through bounding assumptions in TH^2 models (e.g., change of micro- and macro-fractures in EDZ). Comparisons will be made against predictions in step 2, including parameter uncertainty associated with new parameters and sensitivity of key parameters through time.

A proposed schedule for these tasks is presented in the following table. There is planned overlap between steps to allow some flexibility in the progress of different teams.

Table 3. Proposed detailed Task E schedule of steps.

	Apr.	Nov.	Apr.	Nov.	Apr.	Nov.	Apr.	Nov.
	2020		2021		2022		2023	
Step 0								
Step 1								
Midterm Report → (Nov 2021)								
Step 2								
Step 3								
					Papers and Final Report → (Nov 2023)			

An interim and final task technical report will be produced (two heavy vertical lines), soon after the corresponding November workshops. Teams participating in the Task will be asked to write short technical reports on the completion of relevant steps, which will feed into these two reports. Specific deadlines will be given for each milestone report at least 6 months in advance.

The final period (April-Nov 2023) will focus on wrapping all the previous steps, organizing and preparing journal manuscripts, and preparing the final DECOVALEX Task E report.

4. Data

At first (until the DECOVALEX internal filesharing system is available) published reports and data will be available via the following Google Drive folder

https://drive.google.com/drive/folders/17rmwesxVqsTDFM-WR6Fo2TZ-QVNYkY9k?usp=sharing

Sandia National Laboratories policy states Google Drive can only be used for distributing final published data and existing reports that have been through proper review and approval channels. Unpublished or working data may only be distributed by email.

Once the project file sharing system is available, this Google Drive link will be replaced, and all the content will be moved to the project file share.

This shared folder already includes or will include:

- Key journal papers and lab reports cited in this specification, upon which the study is based
- Spreadsheets of WIPP brine inflow data from Finley et al. (1992) and Deal et al. (1995)
- BATS field data, laboratory data, relevant test description details from reports and laboratory notebooks
- Presentations and reports from the DECOVALEX-2023 workshops
- Revisions of this specification document

Whenever possible, we should use similar SI units to make comparison of results simpler

- Meters
- Seconds
- Grams
- Celsius

Unpublished BATS data will be shared among the group, but this data must not be distributed externally beyond the DECOVALEX-2023 Task E participants, until it is ready for report, journal, or conference proceedings publication, and has been through the required review and approval process. We will discuss as a group what approach works best for all participants.

5. Step 0 – Detailed Requirements

5.1 Requirements

Teams are requested to perform the following work to facilitate comparison between teams and to gradually build the understanding of the data, coupled physics, and related sensitivity and uncertainty. The requirements in this step should build familiarity with the WIPP setting, the BATS field test, the thermal/hydrological behavior of bedded salt, and the estimation of parameter uncertainty and sensitivity, without introducing too many complexities.

1. Simulate brine production through time to any three of the 17 WIPP boreholes monitored as part of the small-scale brine inflow test (Finley et al., 1992; Appendix E). Data are in spreadsheet form on the file sharing site. The data initially include weekly (and later monthly) brine masses pumped out of sealed boreholes soon after their completion. Some of these data can be matched well using single-phase (brine only) flow down a pressure gradient (i.e., atmospheric pressure in borehole, hydrostatic or lithostatic pressure in the far-field). Some of the boreholes show anomalous increases in production at late time, which require different conceptual models (Webb, 1992). These anomalous data shouldn't be the focus of Step 0. Vertical boreholes may require considering different permeabilities of horizontal layers intersecting the boreholes (e.g., Clay F or Marker Bed 139). Beauheim et al. (1997) summarizes the INTRAVAL investigation, which also used these data. This report includes relevant WIPP geologic and hydrologic background and the results of three participating international teams.

   McTigue (1993, Section 6.2.1) details the data reduction effort (i.e., discarding anomalous data) in their parameter estimation process. This report also presents 1D analytical solutions for flow to boreholes in an infinite cylindrically symmetric porous medium and discusses tips for evaluating the integrals using quadrature (i.e., breaking up the integrals, because the integrals have singularities at one end). Extended-precision or adaptive integration routines (e.g., Mathematica or mpmath) may allow straightforward integration of the solution as written. Gelbard (1992) presents a set of more complex 1D and 2D analytical solutions for flow to a borehole near a drift, considering the finite length of the borehole, a finite domain size (i.e., $k \rightarrow 0$ outside the EDZ), and the effects of the access drift EDZ.

   The small-scale brine inflow experiment involved measuring brine production in boreholes immediately after their construction, mostly in recently mined access drifts. For older access drifts, a larger lag between drilling and monitoring boreholes, or adjacent boreholes with intersecting EDZs can lead to dry out and two-phase flow complications.

2. Simulate the change in temperature around a constant-temperature borehole heat source in salt, from the Jan-Mar 2020 BATS heating cycle. Mills et al. (2019) present the as-built configuration. A large number of thermocouples have time series of temperature every 15 minutes. A constant-temperature boundary condition (~96 ºC, with ~30 ºC pre-test temperature) was applied to a 60-cm interval of the central HP borehole wall (centered at a depth of ~2.9 m into the 12.2-cm diameter borehole) via a controlled 750 W infrared lamp. The temperature field around the heater can be predicted relatively well using conduction only (no convection). Thermocouples are grouted into place along the 5.5-m length of adjacent 4.5-cm diameter boreholes (T1, T2, E1, E2, and E3 boreholes, Figure 8).

   During the first few hours of the thermal test, there were some issues with the heater controller, requiring three attempts to keep the heater on. The notes indicate the start times of relevant events (power on, power off), and the geometry of the boreholes and sensors (local coordinate system for each thermocouple and the heater) will be provided.

Previous lab estimates of the thermal conductivity of WIPP salt and for single-crystal halite (Sweet & McCreight, 1981; Bauer & Urquhart, 2014) show the thermal conductivity of salt is about $5\,\frac{\mathrm{W}}{\mathrm{m}\cdot\mathrm{K}}$ and slightly non-linear (decreasing thermal conductivity with T, but uniform heat capacity with T of about $2 \times 10^6\,\frac{\mathrm{J}}{\mathrm{m}^3\cdot\mathrm{K}}$). This non-linearity may or may not be important over the range of temperatures experienced by the salt in this experiment (~66 ºC change).

Laboratory estimates of thermal conductivity and heat capacity over the temperature range 30 to 150 ºC are being made at SNL for core samples from the BATS test array (cores from HP and SL boreholes), and for samples of the grout used to set the thermocouples into the T and E boreholes. These lab data will be provided to Task E participants once tests are complete (testing is underway in April 2020).

Models may have homogeneous properties, or they may include the effects of grouted and open boreholes. Models can be 1D spherically symmetric infinite-domain analytical solutions (e.g., §9.10 of Carslaw & Jaeger, 1959 or §6.5 of Crank, 1975) or can be gridded numerical models including the effects of the geometry of boreholes and the drift. Models should fit at least 5 observation locations through time, including heating and cooling (either separately or together, but using the same material properties).

There is some uncertainty about the actual borehole wall temperature (~96 ºC fits the data better than the set temperature of 120 ºC, which may be due to the lamp shining directly on the controlling thermocouple), so it may be worthwhile to also estimate the borehole wall temperature.

3. Model simulations of brine production and temperature in bullets 1 and 2 above should include quantification of relative uncertainty in parameter estimates. The method of parameter estimation (e.g., Levenberg-Marquardt algorithm, Nelder-Mead algorithm, or Markov-chain Monte Carlo), and the method for uncertainty quantification are not specified, but they should address the relative uniqueness of the predicted best-fit parameters, in light of the observed data. Near optimal fit (in parameter "space"), the linearized parameter sensitivity to observations through time will be estimated. A linearized and straightforward way of doing this is by independently perturbing each parameter (e.g., Δ 1%), then quantifying the resulting change in prediction at each time (i.e., a finite-difference approximation to a Jacobian matrix).

   PEST is a free software implementation of the Levenberg-Marquardt parameter estimation algorithm that also provides scaled sensitivity results (Doherty, 2015). DAKOTA is an open-source suite of algorithms for uncertainty quantification, parameter estimation, and sensitivity analysis (Adams et al., 2014).

Generally, in diffusive systems (e.g., heat conduction, single-phase Darcy flow) it is *characteristic* to plot change in primary variable against change in time on a log-log scale. Adjusting parameters to get the right "shape" of the response in log-log space can be more fruitful than fitting the data in an average absolute value sense on linear scale. Often the transient properties of the system are most sensitive to relatively few early-time observations, which may be "lost" in the lower-left corner of linear-linear plots. In more complex models, the derivative of the model is fit also to the derivative of the data, to ensure shape information is captured in the objective function (e.g., Bourdet, 2002). Likewise, during parameter estimation, the analyst may need to winnow late-time data (e.g., linear spacing will significantly over-represent late-time data in a uniformly weighted objective function), non-uniformly weight the data, or otherwise carefully treat the system to improve estimability of all parameters.

5.2 Deadlines

There are no specific individual deadlines for reporting the results of Step 0, but it will be described along with Step 1 in the midterm report due soon after the November 2021 workshop.

6. Step 1 – Detailed Requirements

6.1 Requirements

Teams are requested to benchmark numerical models against a published analytical TH[1] solution and to make the step from single-phase (H[1]) to two-phase (H[2]) hydrological flow.

1. Benchmark numerical models to be used in this and subsequent steps with an analytical thermoporoelasticity solution (TH[1]) for 1D cylindrically symmetric flow to a borehole in an infinite medium (McTigue, 1990). The comments from Step 0 regarding evaluation of the integrals also apply here (e.g., see McTigue, 1993). This analytical solution includes the effects of solid and liquid phase thermal expansion, and flow towards an infinitely long borehole in an infinite medium under a pressure gradient. Both the analytical solution and numerical models should be parameterized with the physical properties for salt presented in Table 1 of McTigue (1986). For reference, related analytical solutions to the same physical problem with different boundary conditions or limiting assumptions are presented in Chen (2016; Chapter 11).

   Comparison between the numerical model and the analytical solution should be made along two profiles: a profile through several log cycles of time at a single location (one borehole radius into the salt), and a profile through space, at a single time (before boundary effects are encountered in the numerical model). This comparison may require simplifying some equations of state in numerical models (e.g., changes in fluid viscosity or thermal conductivity with T, which the analytical solution doesn't account for).

   All modifications or simplifications required to match the analytical solution should be documented, and the effects of these non-linearities on the prediction should be compared with the analytical solution. Plot numerical model solution with and without non-linear effects against the analytical solution, as a function of space and time.

2. Multi-phase (unheated) flow (H[2]) to a borehole in salt requires several additional parameters, beyond those in Step 0. Data on capillary pressure (p_c) vs. liquid saturation (S_e) are published for fine granular salt (Cinar et al., 2006; Olivella et al., 2011), and two-phase flow characterization data exist for the meter-scale clay and anhydrite bed MB-139 at WIPP (Howarth & Christian-Frear, 1997), but these are not completely relevant to two-phase flow in the EDZ. One or more approaches should be documented to choosing functional form and required parameters for p_c and related relative permeability (k_r) vs. S_e curves relevant to an EDZ surrounding a drift and boreholes in salt (i.e., BATS).

   Brine imbibition tests (analogous to those done in tuff by Peters et al., 1987) will be conducted on dry core samples from BATS boreholes. The data (mass of brine imbibed through time) can be used with a H[2] numerical model to constrain p_c and k_r models. Models could also be constrained from pore network models derived from CT scan data (Figure 4; Betters et al., 2020), or using published data from other rock types (Davies, 1991).

   Uncertainty should be quantified associated with whichever parameterization method was chosen. For example, model-data uncertainty from laboratory imbibition data, uncertainty in using p_c models for continuum models from CT-derived pore network models, and uncertainty in the range of possible literature values for different rock types.

3. Simulations of the initial conditions for the BATS heater test will be developed (i.e., H[2]/H[2]M flow in a salt EDZ accounting in some way for the development of damage and the dry-out effects of the drift and boreholes). Numerical models may explicitly include two-phase flow or use Richards' approximation. Permeability in the EDZ may be anisotropic (i.e., $k_r \ll k_\theta$, Figure 3) to reflect the orientation of microfractures observed in cores (Figure 4). The N-940 drift, where BATS is located, was mined in 2012 and the boreholes for the BATS test were drilled in

February-April 2019 (Mills et al., 2019). Simulations of brine production will be compared to limited observations of brine production in BATS instrument boreholes before grouting and from N_2 circulation in the unheated BATS array.

Uncertainty associated with H^2 flow predictions to boreholes will be assessed. Either associated with *a priori* assumed distribution of hydrologic parameters (e.g., extent of EDZ, zoned or graded EDZ, correlations between the hydrologic EDZ properties: ϕ, k, and air-entry pressure) or a H^2M-derived distribution of parameters from mechanical damage. Sensitivity of key parameters on brine production predictions will be quantified through time.

6.2 Deadlines

The results of Steps 0 and 1 will be described in the midterm report, to be prepared by the task lead soon after the November 2021 workshop. Participants should provide draft material on their contribution prepared and submitted to the task lead for incorporation into the midterm report by the beginning of the 2021 holiday break.

7. Step 2 – Detailed Requirements

7.1 Requirements

Teams are requested to produce TH^{2}M results related to extending the two-phase flow initial conditions in Step 1 with the addition of temperature distribution around a heat source, and any T-M related coupling. Optionally, this will include simulation of gas and liquid breakthrough in unheated and heated tracer tests. *Revision 0 of the Task E specification has a preliminary description of this step.*

1. We seek to recreate the observed circumstance where significant amount of brine enters a heated borehole after the end of heating. This effect has been documented several times (Figure 10) but has also been dismissed as "unimportant" to radioactive waste disposal, since it is believed this is a peculiarity of turning off a man-made (i.e., non-radioactive) heat source. For radioactive waste, the decrease in thermal power through time may be slow enough for viscoplastic creep to eliminate any differential thermal stresses that arise (e.g., ^{137}Cs and ^{90}Sr have ~30-yr half-lives). Despite this, we feel understanding the effect thermo-mechanical stresses have on ϕ and k will allow better prediction of relatively reduced brine production observed during the heating phase. It is believed the spike of brine production during cooling phase provides a much better calibration target than the reduced brine inflow observed during the heating phase, and the same physical model should predict both processes.

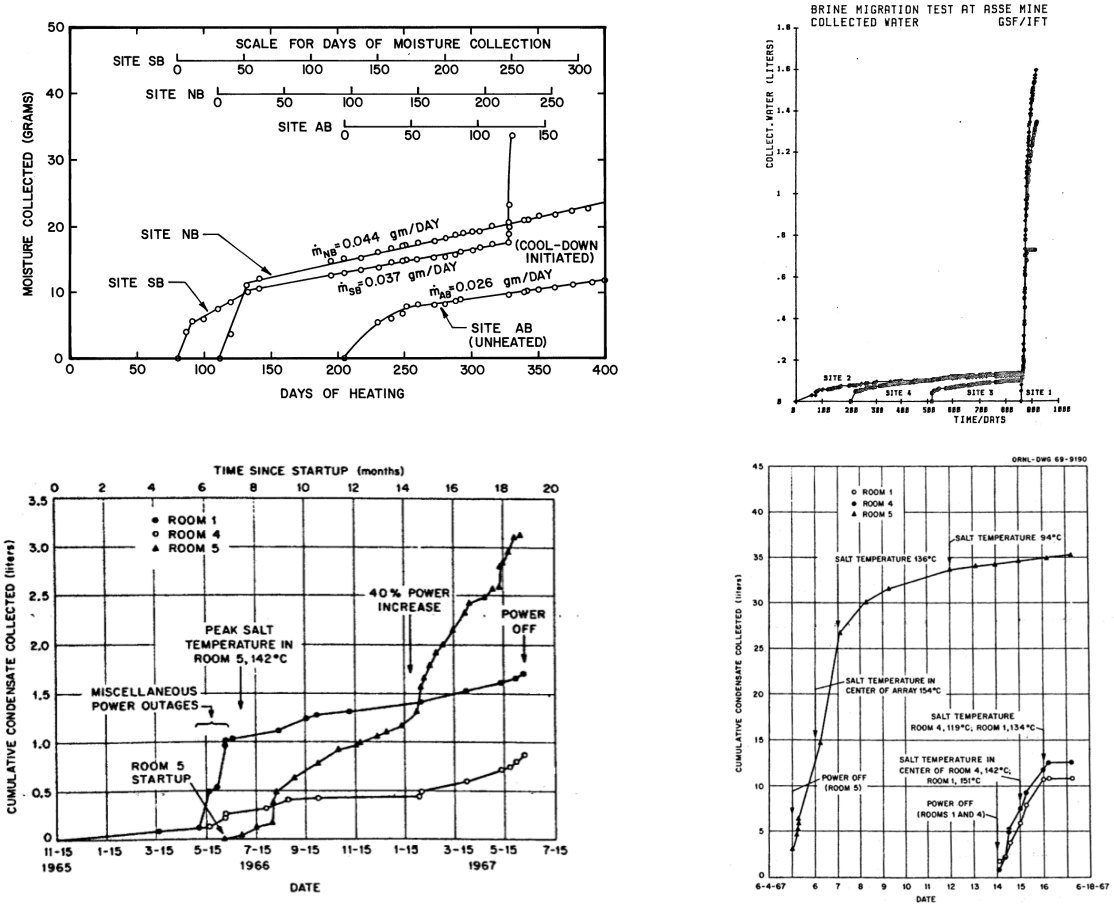

Figure 10. Example brine production spikes after end of heating at Avery Island (top left: Krause, 1983), Asse (top right: Rothfuchs et al., 1988), and Project Salt Vault (bottom: Bradshaw & McClain, 1971) field-scale heated brine-migration tests.

One possible approach is to extend the conceptual model embodied by McTigue's (1986; 1990) thermoporoelasticity solution, including changes in ϕ and k. Generally, increases in confining stress will close EDZ fracture ϕ and reduce EDZ k, while increases in shear stress (beyond the dilatancy criteria) will increase damage, ϕ, and k in salt (Sutherland & Cave, 1978; Stormont & Fuenkajorn, 1993; Pfeifle et al., 1998). Increases in temperature lead to thermal expansion of the solid and liquid phases, with the resulting change in stress state leading to a subsequent change in absolute permeability (Figure 11).

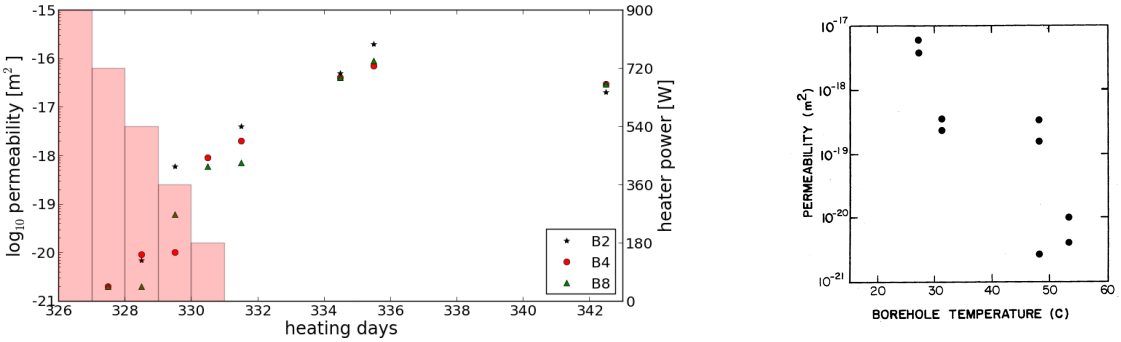

Figure 11. Observed changes in gas permeability of salt during stepped cool-down phase of Avery Island brine migration test (left: data from Krause, 1983) and permeability of drift EDZ at different temperatures (right: Stickney & Van Sambeek, 1984).

Beyond the single-phase flow conceptual model of McTigue, k_r in salt can further be modified because quickly closing fractures filled with a mixture of air and brine will increase brine saturation, due to the higher compressibility and mobility of gas. Capillarity may also be modified by changes in temperature, since liquid surface tension decreases with temperature.

Brine production spikes significantly immediately after shutting off the heater (Figure 10), related to contraction of salt, reduction of stress (stress state possibly even becoming tensile in places), and likewise increase in porosity and permeability. Before turning off the heater, brine has increased pressure due to thermal expansion (and likely thermal pressurization, associated with decreases in permeability during heating). Increased permeability near the borehole at heater shutdown allows the high-pressure brine to more readily flow towards the borehole. At Avery Island nearly as much brine flowed into the borehole during the week following heating, as the previous >200 days of heating (Figure 10). In the brine migration tests at Asse (domal) and during Project Salt Vault (bedded salt, with significantly more non-salt shale interbeds in Room 5), approximately 90% of the total brine inflow in the experiment came during the shutdown of the heaters. In both domal field tests, the heater power was stepped down over several days in an attempt to reduce this effect, with limited effect. A similar result was observed after the Jan-Mar 2020 heating episode at BATS.

Gas packer permeability tests will be conducted in the heated BATS array during heating and cooling, to document apparent gas permeability of the salt in the EDZ during temperature changes. Laboratory tests also be conducted to document the gas permeability of the salt as a function of temperature and confining stress.

2. Optionally, simulate advection in liquid and gas tracer tests conducted between D, HP, and SM boreholes in the *unheated* BATS array. Simulations of tracer breakthrough will be fit to observations. These tracer tests will allow better quantification and assessment of transport properties across the EDZ. Uncertainty and parameter sensitivity should be addressed.

3. Optionally, simulate advection in liquid and gas tracer tests conducted between the D, HP, and SM boreholes in the *heated* BATS array. Simulations of tracer breakthrough will be fit to observations. These tracer tests will allow better quantification and assessment of transport properties across the EDZ. Uncertainty and parameter sensitivity should be addressed.

7.2 Deadlines

There are no specific individual deadlines for reporting the results of Step 2, but it will be described along with the rest of the task in the final report due soon after the November 2023 workshop.

8. Step 3 – Detailed Requirements

8.1 Requirements

Teams are requested to performed model predictions associated with one or more of the following optional BATS test case data sets. *Revision 0 of the Task E specification has a preliminary description of this step*.

This step includes 4 alternatives; choose one or more of interest.

A. Simulate TH^2M brine production using geophysical data as constraints. Using time-lapse ERT and/or AE timing and source location estimates, constrain TH^2M brine production estimates from step 2. ERT results show changes in resistivity, which can be related to changes in brine content (given changes in resistivity with temperature are estimable) from steps 1 and 2. AE reveals the timing and location of cracking in the salt, which can constrain or confirm predicted changes in k due to changes in σ in step 2. Compare the parameter uncertainty and sensitivity estimates from previous steps.

B. Simulate TH^2MC cement seal permeability in lab/field. Predict (i.e., no field seal permeability data exist to compare against) permeability of the confined borehole salt/cement system in heated and unheated SL boreholes from observed temperature, strain, and post-test compositional analyses. GRS will provide poromechanical lab test results (including permeability of a salt/seal/brine system) using WIPP salt and brine, along with similar cement recipes. Present uncertainty in model parameters and sensitivity of key parameters to observations through time.

C. Simulate TH^2MC brine production with additional geochemical processes. Brine production estimates from step 2 will be updated to include one or more of the following more complex H^2C effects:

    a. distribution and behavior of different water sources (i.e., fluid inclusions, clay dehydration) in multi-phase brine inflow predictions (Jordan et al., 2015; Hu & Rutqvist, 2020);

    b. effects from precipitation and dissolution of salt on k and ϕ;

    c. brine composition changes in time (e.g., ionic content of produced brine from different water sources) and mineralogical content of precipitated salts;

    d. non-condensable gas composition of produced gas stream; and

    e. isotopic composition of produced water (i.e., including laboratory data from LANL on the isotopic makeup of different water types in salt).

    Comparisons will be made against predictions in step 2, including parameter uncertainty and sensitivity of key parameters through time.

D. Simulate TH^2M brine production with creep. Creep closure in salt is driven by and works to reduce differential stresses. Creep becomes more significant at longer time scales, higher deviatoric stresses, and higher temperatures. This additional mechanism should either be considered explicitly in coupled viscoplastic numerical models or through bounding assumptions in TH^2 models (e.g., change of micro- and macro-fractures in EDZ). Comparisons will be made against predictions in step 2, including parameter uncertainty associated with new parameters and sensitivity of key parameters through time.

8.2 Deadlines

The results of Steps 2 and 3 will be described in the final report, to be prepared by the task lead soon after the November 2023 workshop. Participants need to have draft material on their contribution prepared and submitted to the task lead for incorporation into the midterm report by the 2023 holiday break.

9. References

Adams, B.M., M.S. Ebeida, M.S. Eldred, J.D. Jakeman, L.P. Swiler, J.A. Stephens, D.M. Vigil, T.M. Widey, W.J. Bohnhoff, K.R. Dalbey, J.P. Eddy, K.T. Hu, L.E. Bauman & P.D. Hough, 2014. *Dakota, A Multilevel Parallel Object-Oriented Framework for Design Optimization, Parameter Estimation, Uncertainty Quantification, and Sensitivity Analysis: Version 6.0 User's Manual*, (331 p.) SAND2014–4633. Albuquerque, NM: Sandia National Laboratories.

Bauer, S.J. & A. Urquhart, 2014. *Thermophysical Properties of Reconsolidating Crushed Salt* (93 p.), SAND2014–2240. Albuquerque, NM: Sandia National Laboratories.

Beauheim, R.L., A. Ait-Chalel, G. Vouille, S.-M. Tijani, D.F. McTigue, C. Brun-Yaba, S.M. Hassanizadeh, G.M. van der Gissen, H. Holtman & P.N. Mollema, 1997. *INTRAVAL Phase 2 WIPP 1 Test Case Report: Modeling of Brine Flow Through Halite at the Waste Isolation Pilot Plant Site*, (124 p.) SAND97–0788. Albuquerque, NM: Sandia National Laboratories.

Beauheim, R.L. & R.M. Roberts, 2002. Hydrology and hydraulic properties of a bedded evaporite formation, *Journal of Hydrology, 259*(1–4):66–88.

Betters, C., J. Vornlocher, T. Paronish, D. Crandall, J. Moore & K.L. Kuhlman, 2020. *Computed Tomography Scanning and Geophysical Measurements of the Salado Formation from Boreholes at the Waste Isolation Pilot Plant*, (44 p.) NETL-TRS-1-2020. Morgantown, WV: National Energy Technology Laboratory.

Borns, D.J. & J.C. Stormont, 1988a. *An Interim Report on Excavation Effect Studies at the Waste Isolation Pilot Plant: The Delineation of the Disturbed Rock Zone*, (35 p.) SAND87–1375. Albuquerque, NM: Sandia National Laboratories.

Borns, D.J. & J.C. Stormont, 1988b, *The Delineation of the Disturbed Rock Zone Surrounding Excavations in Salt*, (8 p.) SAND88-2230C. Albuquerque, NM: Sandia National Laboratories.

Boukhalfa, H. P.J. Johnson, D. Ware, D.J. Weaver, S. Otto, B.L. Dozier, P.H. Stauffer, M.M. Mills, E.N. Matteo, N.B. Nemer, C.G. Herrick, K.L. Kuhlman, Y. Wu & J. Rutqvist, 2018. *Implementation of Small Diameter Borehole Thermal Experiments at WIPP*, (70 p.) LA-UR-18–29203. Los Alamos, NM: Los Alamos National Laboratory.

Bourdet, D., 2002. *Well Test Analysis: The Use of Advanced Interpretation Models*, Elsevier.

Bradshaw, R.L. & W.C. McClain, 1971. *Project Salt Vault: A Demonstration of the Disposal of High-Activity Solidified Wastes in Underground Salt Mines,* (374 p.) ORNL-4555. Oak Ridge, TN: Oak Ridge National Laboratory.

Carslaw, H.S. & J.C Jaeger, 1959. *Conduction of Heat in Solids*, second edition, Oxford.

Cheng, A.H.-D., 2016. *Poroelasticity*, Springer.

Cinar, Y., G. Pusch & V. Reitenbach, 2006. Petrophysical and capillary properties of compacted salt, *Transport in Porous Media, 64*(2):199–228.

Crank, J., 1975. *The Mathematics of Diffusion*, second edition, Oxford.

Czaikowski, O., J. Dittrich, U. Hertes, K. Jantschik, K. Wieczorek & B. Zehle, 2016. *Full Scale Demonstration of Plugs and Seals (DOPAS): Final Technical Report on ELSA Related Testing on Mechanical-Hydraulical Behavior - LASA*, (119 p.) GRS-A-3851. Braunschweig, Germany: Gesellschaft für Anlagen- und Reaktorsicherheit (GRS).

Davies, P.B., 1991. *Evaluation of the Role of Threshold Pressure in Controlling Flow of Waste-Generated Gas into Bedded Salt at the Waste Isolation Pilot Plant*, (62 p.) SAND90–3246. Albuquerque, NM: Sandia National Laboratories.

Davies, C. & F. Bernier, 2005. *Impact of the Excavation Disturbed or Damaged Zone (EDZ) on the Performance of Radioactive Waste Geologic Repositories*, (359 p.) EUR 21028 EN. Luxembourg: European Commission Nuclear Science and Technology.

Deal, D.E., R.J. Abitz, D.S. Belski, J.B. Case, M.E. Crawley, C.A. Givens, P.P.J. Lipponer, D.J. Milligan, J. Meyers, D.W. Powers & M.A. Valdivia, 1995. *Brine Sampling and Evaluation Summary Program 1992-1993 Report and Summary of BSEP Since 1982*, (294 p.) DOE-WIPP 94–011. Carlsbad, NM: Westinghouse Electric Corporation.

Doherty, J., 2015. *Calibration and Uncertainty Analysis for Complex Environmental Problems*, (237 p.) Brisbane, Australia: Watermark Numerical Computing.

Finley, S.J., D.J. Hanson & R. Parsons, 1992. *Small-Scale Brine Inflow Experiments – Data Report Through 6/6/91*, (185 p.) SAND91–1956. Albuquerque, NM: Sandia National Laboratories.

Gelbard, F., 1992. *Exact Analysis of a Two-Dimensional Model for Brine Inflow to a Borehole in a Disturbed Rock Zone*, (109 p.) SAND92–1303. Albuquerque, NM: Sandia National Laboratories.

Guiltinan, E.J., K.L. Kuhlman, J. Rutqvist, M. Hu, H. Boukhalfa, M. Mills, S. Otto, D.J. Weaver, B. Dozier & P.H. Stauffer, 2020. Temperature response and brine availability to heated boreholes in bedded salt, *Vadose Zone Journal* (in press).

Hansen, F.D., 2003. The Disturbed Rock Zone at the Waste Isolation Pilot Plant, (62 p.) SAND2003–3407. Albuquerque, NM: Sandia National Laboratories.

Howarth, S.M. & T. Christian-Frear, 1997. P*orosity, Single-Phase Permeability, and Capillary Pressure Data from Preliminary Laboratory Experiments on Selected Samples from Marker Bed 139 at the Waste Isolation Pilot Plant*, (3 vol.) SAND94–0472. Albuquerque, NM: Sandia National Laboratories.

Hu, M. & J. Rutqvist, 2020. Finite volume modeling of coupled thermo-hydro-mechanical processes with application to brine migration in salt. *Computational Geosciences* (in press).

Johnson, P.J., S.M. Bourret, H. Boukhalfa, F.A. Caprouscio, G.A. Zyvoloski, D.J. Weaver, S. Otto, M.M. Mills, E.M. Matteo, K.L. Kuhlman, J. Rutqvist, Y. Wu & P.H. Stauffer, 2017. *Test Plan Document for Thermal Testing in Salt*, (45 p.) LA-UR-1730762. Los Alamos, NM: Los Alamos National Laboratory.

Johnson, P.J., S. Otto, D.J. Weaver, B. Dozier, T.A. Miller, A.B. Jordan, N. Hayes-Rich & P.H. Stauffer, 2019. Heat-generating nuclear waste in salt: field testing and simulation, *Vadose Zone Journal, 18*(1):1-14.

Johnson, P.J., G.A. Zyvoloski & P.H. Stauffer, 2019. Impact of a porosity-dependent retention function on simulations of porous flow, *Transport in Porous Media, 127*(1):211-232.

Jordan, A.B., H. Boukhalfa, F.A. Caporuscio; B.A. Robinson & P.H. Stauffer, 2015. Hydrous mineral dehydration around heat-generating nuclear waste in bedded salt formations, *Environmental Science & Technology, 49*(11):6783-6790.

Krause, W.B., 1983. *Avery Island Brine Migration Test: Installation, Operation, Data Collection, and Analysis,* (91 p.) ONWI-190(4). Rapid City, SD: RE/SPEC Inc.

Kuhlman, K.L., 2019. *Processes in Salt Repositories,* (41 p.) SAND2019-6441R. Albuquerque, NM: Sandia National Laboratories.

Kuhlman, K.L., 2014. *Summary Results for Brine Migration Modeling Performed by LANL, LBNL, and SNL for the UFD Program,* (105 p.) SAND2014–18217R. Albuquerque, NM: Sandia National Laboratories.

Kuhlman, K.L., C.M. Lopez, M.M. Mills, J.M. Rimsza & D.C. Sassani, 2018. *Evaluation of Spent Nuclear Fuel Disposition in Salt (FY18)*, (83 p.) SAND2018–11355R. Albuquerque, NM: Sandia National Laboratories.

Kuhlman, K.L. & B. Malama, 2013. *Brine Flow in Heated Geologic Salt* (128 p.), SAND2013–1944. Albuquerque, NM: Sandia National Laboratories.

Kuhlman, K.L., M.M. Mills, E.N. Matteo, 2017. *Consensus on Intermediate Scale Salt Field Test Design*, (96 p.) SAND2017–3179R. Albuquerque, NM: Sandia National Laboratories.

Lai, C.-S., 1971. *Fluid Flow through Rock Salt Under Various Stress States*, (144 p.) PhD. Dissertation Michigan State University.

McTigue, D.F., 1986. Thermoelastic response of fluid-saturated porous rock, *Journal of Geophysical Research, 91*(B9):9533–9542.

McTigue, D.F., 1990. Flow to a heated borehole in porous, thermoelastic rock: analysis, *Water Resources Research, 26*(8):1763–1774.

McTigue, D.F., 1993. *Permeability and Hydraulic Diffusivity of Waste Isolation Pilot Plan Repository Salt Inferred from Small-Scale Brine Inflow Experiments*, (91 p.) SAND92–1911. Albuquerque, NM: Sandia National Laboratories.

Mills, M., K. Kuhlman, E. Matteo, C. Herrick, M. Nemer, J. Heath, Y. Xiong, C. Lopez, P. Stauffer, H. Boukhalfa, E. Guiltinan, T. Rahn, D. Weaver, B. Dozier, S. Otto, J. Rutqvist, Y. Wu, M. Hu & D. Crandall, 2019. *Salt Heater Test (FY19)*, (61 p.) SAND2019–10240R. Albuquerque, NM: Sandia National Laboratories.

Nowak, E.J. & D.F. McTigue, 1987. *Interim Results of Brine Transport Studies in the Waste Isolation Pilot Plant (WIPP)*, (86 p.) SAND87–0880. Albuquerque, NM: Sandia National Laboratories.

Nowak, E.J., D.F. McTigue & R. Beraun, 1988. *Brine Flow to WIPP Disposal Rooms: Data, Modeling and Assessment*, (82 p.) SAND88–0112. Albuquerque, NM: Sandia National Laboratories.

Olivella, S., S. Castagana, E.E. Alonso & A. Lloret, 2011. Porosity variations in saline media induced by temperature gradients: experimental evidences and modelling. *Transport in Porous Media, 90*(3):763–777.

Peters, R.R., E.A. Klavetter, J.T. George & J.H. Gauthier, 1987. "Measuring and Modeling Water Imbibition into Tuff", pp. 99–106 *in* Evans, D.D. & T.J. Nicholson [Eds], *Flow and Transport Through Unsaturated Fractured Rock*, (187 p.) AGU Geophysical Monograph 42, Washington DC: American Geophysical Union.

Pfeifle, T.W., N.S. Brodsky & D.E. Munson, 1998. *Experimental Determination of the Relationship Between Permeability and Microfracture-Induced Damage in Bedded Salt*, (10 p.) SAND98–0411C. Albuquerque, NM: Sandia National Laboratories.

Popp, T., 2019. "Natural Closure of Salt Openings", pp. 262–280 *in* Buchholz, S., E. Keffeler, K. Lipp, K. DeVries & F. Hansen [Eds], *Proceedings of the 10th US/German Workshop on Salt Repository Research, Design, and Operation*, (790 p.) SAND2019–9997R, Albuquerque, NM: Sandia National Laboratories.

Rothfuchs, T., K. Wieczorek, H.K. Feddersen, G. Staupendahl, A.J. Coyle, H. Kalia & J. Eckert, 1988. *Brine Migration Test Final Report*, (317 p.) GSF-Bericht 6/88, Remlingen, F.R. Germany: Gesellschaft für Strahlen- und Umweltforschung mbH München (GSF).

Stauffer, P.H., A.B. Jordan, D.J. Weaver, F.A. Caporuscio, J.A. Tencate, H. Boukhalfa, B.A. Robinson, D.C. Sassani, K.L. Kuhlman, E.L. Hardin, S.D. Sevougian, R.J. MacKinnon, Y. Wu, T.A. Daley, B.M. Freifield, P.J. Cook, J Rutqvist & J.T. Birkholzer, 2015. *Test Proposal Document for*

Phased Field Testing in Salt, (104 p.) LA-UR-15-23154, Los Alamos, NM: Los Alamos National Laboratory.

Stickney, R.G. & L.L. Van Sambeek, 1984. *Summary of the Avery Island Field Testing Program* (75 p.), RSI-0225. Rapid City, SD: RE/SPEC Inc.

Stormont, J.C. & K. Fuenkajorn, 1993. *Dilation-Induced Permeability Changes in Rock Salt*, (7 p.) SAND93–2670C, Albuquerque, NM: Sandia National Laboratories.

Stormont, J.C., C.L. Howard & J.J.K. Daemen, 1991. *In Situ Measurements of Rock Salt Permeability Changes Due to Nearby Excavations*, (81 p.) SAND90–3134. Albuquerque, NM: Sandia National Laboratories.

Sutherland, H.J. & S. Cave, 1978. *Gas Permeability of SENM Rock Salt*, (42 p.) SAND78–2287. Albuquerque, NM: Sandia National Laboratories.

Sweet, J.N. & J.E. McCreight, 1980. *Thermal Properties Measurement on Rocksalt Samples from the Site of the Proposed Waste Isolation Pilot Plant,* (79 p.) SAND80–709. Albuquerque, NM: Sandia National Laboratories.

Webb, S.W., 1992. *Brine Inflow Sensitivity Study for Waste Isolation Pilot Plant Boreholes: Results of One-Dimensional Simulations*, (234 p.) SAND91–2296. Albuquerque, NM: Sandia National Laboratories.